

WETTING PERFORMANCE AND PRESSURE DROP OF STRUCTURED PACKINGS: CFD AND EXPERIMENT

A. Ataki¹, P. Kolb², U. Bühlman², H.-J. Bart^{1,*}

¹TU Kaiserslautern, Thermische Verfahrenstechnik, POB 3049, D-67653 Kaiserslautern, Germany

²Kühni AG, CH-4123, Allschwil, Switzerland

The wetting performance of a structured packing element of Rombopak 4M (TM Kühni, CH) has been studied experimentally and by computational fluid dynamics (CFD) simulations at different liquid loads ($12 \div 50 \text{ m}^3/\text{m}^2\text{h}$) and liquids varying in their properties (surface tension, viscosity and contact angle). Dyed glycerine-water (with and without surfactant) and chlorobenzene-ethylbenzene liquid mixtures, have been used in the experiments. The experimental evaluation (spreading, wetting) was performed by optical methods. Film thickness was measured by an optical method using a sensor and the contact angle was evaluated by a CCD camera. The VOF (Volume of Fluid) model of Fluent has been used for simulation. After a first confirmation on a simple planar geometry a typical lamella has been investigated. This has been further extended to a block of lamellas representing a packing sheet. The simulations well represent the experimental findings and can be used to derive correlations for liquid hold-up and effective interfacial area at certain system and operating conditions. Additionally, the dry pressure drop is calculated separately, thus virtual experiments reveal the local hydrodynamics in complex geometries. In the presentation a comparison with simulations and experimental data will be given and correlations derived, describing the hydraulic behaviour.

KEYWORDS: CFD, VOF model, Structured packing, Wetting, Two-phase flow, Rombopak, Pressure drop

INTRODUCTION

In the recent years, there has been considerable academic and industrial interest in using CFD methods to simulate the multiphase flows found in industrial applications. Wetting of a solid surface with liquids is considered as an open or free surface liquid flow. It is especially important in packed columns used in chemical engineering, such as distillation, absorption, desorption and others. In vacuum operated columns, which generally work at low liquid loads, the wetting degree plays an important role in enhancement of the heat and mass transfer between the gas and liquid phases. In spite of the development of the CFD codes, the tracking of two and multiphase flows via CFD methods is still in the starting stage [1]. Few works can be found in the literature, which deal with the CFD simulations of flow in structured packings. Most of these works were performed for estimation the dry pressure drop in a basic element of the packings [2–4]. CFD simulations of wetting of solid surface with liquids can be solved with the multiphase flow VOF model [6].

*bart@mv.uni-kl.de, <http://www.uni-kl.de/LS-Bart/>

This model, which was developed by Hirt [5] is a fixed grid technique for tracking the interface between two or more non-interpenetrated phases. It solves a single set of momentum equations throughout the domain and the resulting velocity field is shared among the phases (for more details s. [6]). Some applications of the VOF-model to simulate the wetting of flat or structured plate surfaces with liquid film flow were reported [2–3,7–8]. Information about the liquid film flow over the surface in these works were used to derive the liquid hold-up or wetting degree in the packings [2–3,8].

In a previous work the rivulet flow on plain solid surface, which is a special case of the film flow, was chosen as a starting point for the validation of CFD results as published in [9,13]. In a further work the hydrodynamic performance of the metal structured packing Rombopak 4M (s. Figure 1), which is a product of the Kuhn company (Switzerland) [14–16], was discussed. CFD simulations of the wetting patterns of a basic element of this packing allow to estimate and correlate the degree of wetting, specific effective area and the liquid hold-up of the packing [17]. Different models describing the performance of packed columns were discussed in comparison [10–12,19] and the flow patterns and wetting degree were validated also experimentally.

CFD simulations were carried out in the current study for the wetting of wavy plates and structured packing sheet consisting of three elements or three nodes (s. Figure 1B and D). The CFD-based model presented in [17] was proved using CFD simulations and experimental data for the wavy packing sheet case. Additional 3D-CFD simulations were performed to derive the dry pressure drop in a single element of Rombopak 4M and 9M types in comparison to the experimental data.

CFD DOMAINS

Grid specifications used in the CFD simulations are summarized in Table 1. For the wavy plate a box was selected. Its basic surface represents the wavy plate with a similar structure of the packing (s. Figure 1A & C). To minimize the simulation time a grid has been used in the CFD calculations with a symmetry plane defined in the middle perpendicular to the

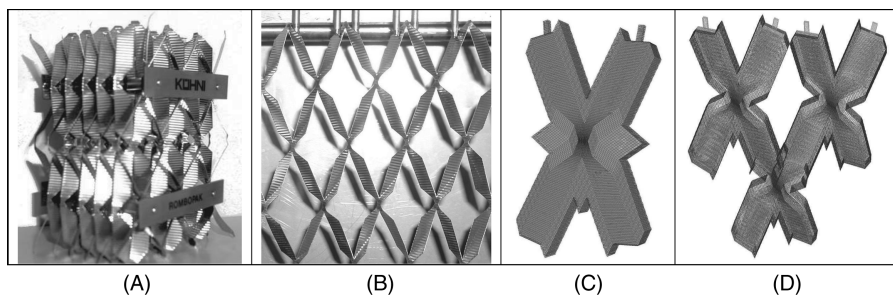


Figure 1. A: Packing block (Rompopak[®] 4M), B: Set of packing elements (a multi-element packing sheet (MS)) C: CFD domain for a single sheet (SS), D: CFD domain for a multi-element sheet (MS)

Table 1. CFD domains for the single (SS) and multi-element packing sheet (MS)

		grid 1 ^a	grid 2 ^b	grid 3 ^c	grid 4 ^b	grid 5 ^c
		box	complex form	complex form	complex form	complex form
Δx	mm	6 ^d	55	90	55	90
Δy	mm	2.5	35	58	26	51
Δz	mm	53	23	45	21	45
D^e	mm	2.5	3	3	1.8	3
grid size	cell	95790	268112	299209	396744	730276
cell size		constant	variable	variable	variable	variable

^aWavy plate, ^bSS, ^cMS, ^dPlate half width, ^eDistance from the wall surface.

plate length. The grid represents in this case a 12 mm width plate. A rectangular channel with liquid velocity inlet was connected at the midpoint of the top plate edge. The liquid flows from the velocity inlet through the channel to form the rivulet flowing on the plate surface. For the structured packing Rombopak 4M a big effort has been spent to represent the fine surface structure of this corrugated element in the CFD simulation of wetting. The grid structure is depicted in Figure 1C with variable cell sizes and the dimensions given in Table 1 (grid 2 & 4). For liquids with low contact angle, surface tension and viscosity, a denser grid (grid 4) was used. The grid used for the packing sheet (grid 3 & 5) was created from one single element and it represents three nodes (s. Figure 1D). The domain height was selected to be higher than the expected maximum liquid film thickness (s. Table 1). For the pressure drop CFD simulations a grid has to be selected which represents the real packing block. The grid shown in Figure 7A was chosen. It is the minimal representative volume of the real packing. Every pair of parallel surfaces was defined as a periodic surface. The flow direction was chosen along the element with a mass flow rate equivalent to the values of the F-factor. Here the pressure drop in a packing element with flat and corrugated plates will be discussed. Tetrahedral cells were chosen for the pressure drop grid and hexahedral for all other grids. All grids have been created using GAMBIT.

EXPERIMENTAL WORK

The experimental set-up to validate the CFD simulations is shown in Figure 2, where the liquid is pumped directly through a pipe (3) (s. Figure 2B) by a gear pump (2) to the liquid distributor (4). Two capillaries feed the liquid to the top lamella of the packing (6) using a metal pipe welded to total of 6 capillaries (5). The liquid flows back from the sump (7) to the reservoir (1). Liquid flow rates can be adjusted by changing the rotating speed of the pump and by the valve (3). Flow rates were measured by weighting the liquid amount within a specific time. An equal liquid distribution at every capillary was achieved in these experiments with a deviation of about 10%. The static contact angle was considered as a constant in the simulations and measured with the well known optical sessile drop method. The experimental set-up for rivulet flow on plates is described elsewhere

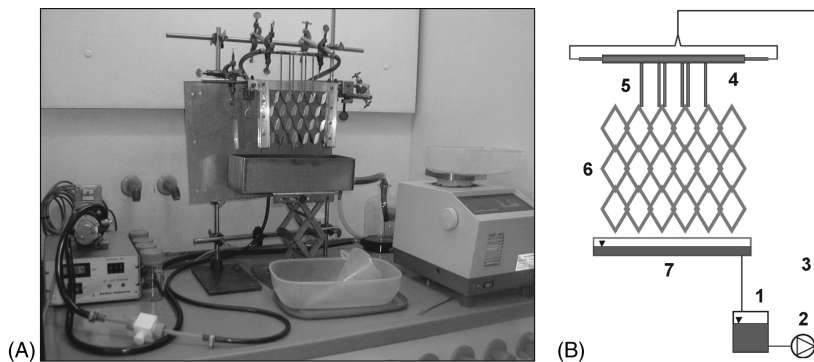


Figure 2. Experimental set-up for wetting of structured packing sheet

[9,13]. For wetting experiments liquids were coloured with dyes to make them easily visible. The dye toluidin blue O, a product of Merck Co., was used for aqueous liquid systems (glycerine water mixtures) and fat red bluish (Sudan Rot R7), a product of Fluka Co., for non aqueous liquids (chlorobenzene-ethylbenzene mixture). We determined the wetting degree by summing up the coloured wetted areas by optical analysis of snap shots for every case. In order to reduce the impact of feed distribution only the lower half of the CFD domain (Figure 1C) is used for analysis.

CFD AND EXPERIMENTAL RESULTS

In the following three different CFD cases will be discussed, as is rivulet flow on an inclined plate, on a structured packing sheet and its dry pressure drop. The rivulet flow was calculated using the VOF model of FLUENT 6.2 [6], where first results with FLUENT 6.0 were given in [9].

RIVULET FLOW ON A WAVY PLATE

VOF contours examples are shown in Figure 3A & B at two flow rates. The evaluation of the rivulets width and maximum thickness was taken at a save distance from the inlet and outlet, where the rivulet is fully developed and no changes were observed. The chosen liquid system was glycerine-water 86.5% and has a viscosity of $\mu_L = 7.54$ mPa.s, contact angle of $\theta = 60^\circ$ and interfacial tension of $\sigma = 60$ mN/m. The rivulet profiles were estimated and found similar to that of the flat plate case [9] and measurements and CFD results are almost similar (Figure 4A). However, there are some deviations when using simplified models derived for flat plates [18]. From the CFD simulations and experimental results it was also found that the rivulet has no linear borderlines. At the crest it constricts and in the dell it extends (s. Figure 3C, 3D). In addition to that the interface was found to be also wavy. Figure 4B shows the locations of the interface at the symmetry ($x = 0$), where the rivulet has its maximum value and two further

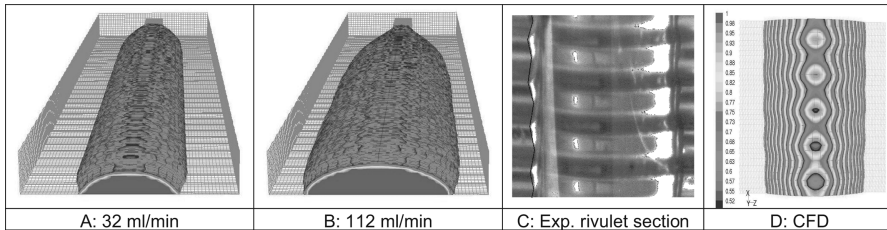


Figure 3. CFD contours on a wavy plate. Plate inclination $\alpha = 68.5^\circ$ Room conditions

positions in a distance 2 respectively 3.5 mm from the symmetry axis. The interface is slightly wavy with similar wave length of the corrugation but lower amplitude.

STRUCTURED PACKING ELEMENT AND PACKING SHEET

Examples of the VOF contours for the flow patterns on SS and MS are shown in Figure 6. The wetted and interfacial areas, in addition to the liquid hold-up are presented as a function of different parameters and are shown graphically in Figure 5. The effect of different parameters can be discussed with help of this figure, where higher liquid flow rate and viscosity leads to higher values. Wetting degree is inversely proportional to the contact angle. Surface tension has smaller effect and increase of the density will decelerate the flow and higher wetted and interfacial area and liquid hold-up are produced. The flow patterns on the bottom part of the packing sheet are very similar to that on the bottom part of the single element cases shown in Figure 6.

The correlations (s. Table 2) developed on a single packing sheet (SS) are also valid for a multi-element packing sheet (MS) with a deviation of 10%. This deviation comes from the fact that the flow pattern is not fully developed in the lower half of the SS (s. Figure 1C) since the liquid redistributes on each packing node. An arrangement of at least 3 packing elements (s. Figure 1D) should be used to minimize the capillary inlet flow effects in order to obtain a fully developed liquid pattern.

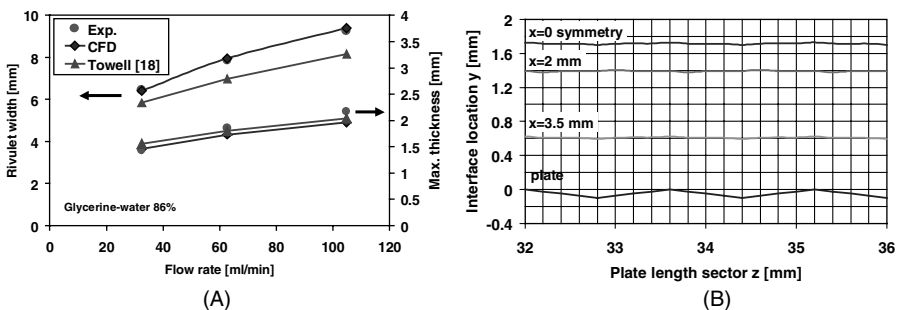


Figure 4. Wavy plate, A: Rivulet width and thickness, B: Interface profiles, 62.5 ml/min

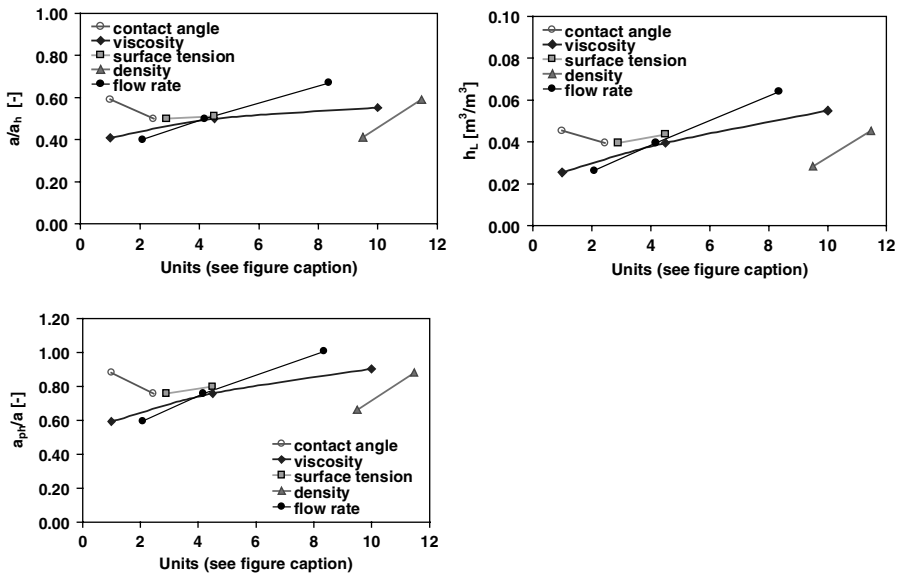


Figure 5. Simulated hydraulic parameters. (Units: contact angle ($^\circ/10$), viscosity (mPasX10), surface tension (mN/m), density ($kg/m^3/10$), flow rate (ml/min))

DRY PRESSURE DROP CFD-SIMULATIONS

Pressure drop is a key factor in the design of packed distillation columns. Structured packings have very complex geometry and the flow inside it cannot be considered as a channel or open flow, which makes the choice of the appropriate turbulent model difficult in the transient region between laminar and turbulent flow. Turbulent flows are significantly

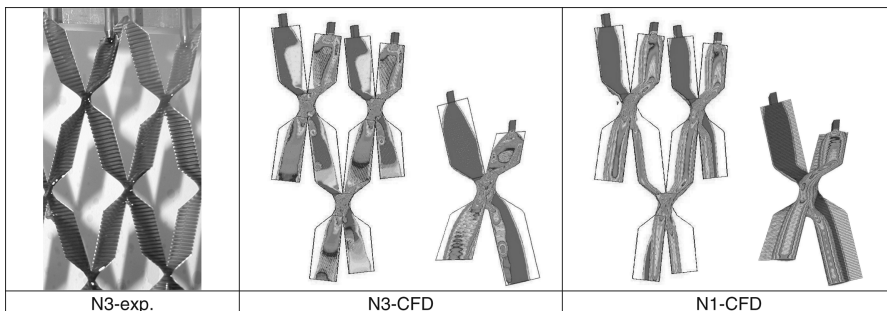


Figure 6. Experimental and CFD contours (SS & MS), N1: grid2/grid3, N3: grid4/grid5

Table 2. Selected structured packing models

Billet [10,19]	CFD-based model [17]
$a_h/a = C_h 0.85 \text{Re}_L^{0.25} Fr_L^{0.1}$	$a_{ph}/a = 1.939 Fr_L^{-0.044} We_L^{0.243} \text{Re}_L^{-0.0266} (\cos \theta)^{0.927}$
$h_L = \left(12 \frac{1}{g} \frac{\mu_L}{\rho_L} u_L a^2\right)^{1/3} \left(\frac{a_h}{a}\right)^{2/3}$	$a_h/a = 1.279 Fr_L^{-0.044} We_L^{0.243} \text{Re}_L^{-0.0266} (\cos \theta)^{0.927}$
C_h : Packing constant	$h_L = 0.675 \left(12 \frac{1}{g} \frac{\mu_L}{\rho_L} u_L a^2\right)^{1/3} \left(\frac{a_h}{a}\right)^{2/3}$

affected by the presence of walls. Obviously, the mean velocity field is affected through the no-slip condition that has to be satisfied at the wall. However, the turbulence is also affected by the packing geometry. The k - ε models are primarily valid for turbulent bulk flows and care has to be taken for wall-bounded flows. In respect to this FLUENT provides both the wall function and the near-wall modelling approach. Enhanced wall treatment is a near-wall modelling method that combines a two-layer turbulent model with enhanced wall functions. If the near-wall mesh is fine enough to be able to resolve the laminar sub-layer, then the enhanced wall treatment will be identical to the traditional two-layer model. This can be done through adoption the cells near the walls (see also [6]).

Different CFD simulations were performed for Rombopak 4M and 9M at different gas loads represented by F-factor (s. Figure 7B and Table 3). The rke (realizable k - ε) turbulent model with ewt (enhanced wall treatment) in FLUENT was used [6]. The pinch, where the lamellas intersect is a critical region. The fine structure for the fine 9M

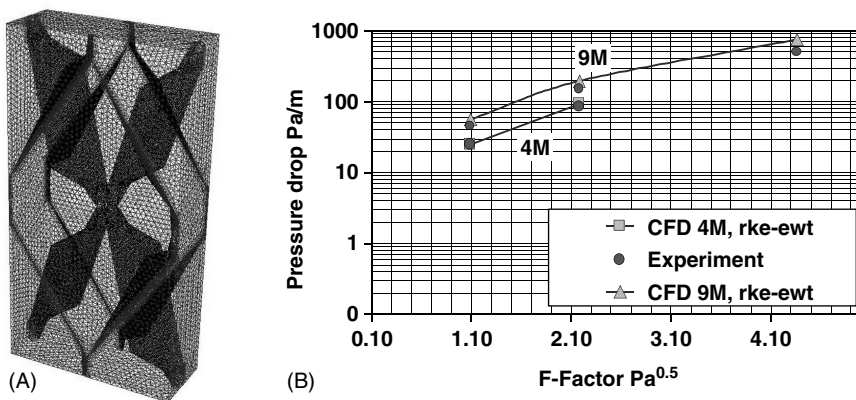
**Figure 7.** A: CFD grid for pressure drop, B: CFD-simulation results

Table 3A. Comparison between the CFD simulation of single (SS) and multi-element packing sheet (MS)

	Re_L	Fr_L	We_L	$\cos\theta$	CFD, SS	CFD, MS	CFD, SS	CFD, MS	CFD, SS	CFD, MS
	$u_L\rho_L/\mu_L a$	$u_L^2 a/g$	$u_L^2\rho_L/\sigma a$	-	a_h/a	a_h/a	a_{ph}/a	a_{ph}/a	h_L	h_L
					-	-	-	-	m^3/m^3	m^3/m^3
N1	4.94	8.49E-04	1.21E-02	0.910	0.552	0.486	0.903	0.784	0.0550	0.0460
N2	50.52	8.88E-04	1.27E-02	0.910	0.409	0.387	0.592	0.604	0.0255	0.0261
N3	141.47	8.50E-04	1.04E-02	0.961	0.521	0.470	0.657	0.606	0.0207	0.0214
N4	10.98	8.49E-04	5.48E-03	0.940	0.565	0.601	0.846	0.905	0.0454	0.0507

N1: $\mu_L = 10$ mPa.s, $\theta = 24.5^\circ$, $\sigma = 29$ mN/m, $\rho_L = 1147$ kg/m³, $Q_L = 41.8$ ml/min. N2: $\mu_L = 1$ mPa.s, $\theta = 24.5^\circ$, $\sigma = 29$ mN/m, $\rho_L = 1147$ kg/m³, $Q_L = 41.8$ ml/min. N3: chlorobenzene-ethylbenzene 50% wt., $\mu_L = 0.3$ mPa.s, $\theta = 16^\circ$, $\sigma = 22.5$ mN/m, $\rho_L = 985$ kg/m³, $Q_L = 41.8$ ml/min. N4: $\mu_L = 4.5$ mPa.s, $\theta = 20^\circ$, $\sigma = 64$ mN/m, $\rho_L = 1147$ kg/m³, $Q_L = 41.8$ ml/min.

packing is very sensitive and small changes in embedding this region in the CFD grid (flat plates SS, Sim6 to 8) gave drastically changes of about 20% in the pressure drop. For the coarse 4M packing the surface structure is negligible, when comparing the cases for corrugated plates (Sim 4 & 5) SS with that for flat SS (Sim 9 & 10). The dry pressure drop simulations for structured 4M SS were found in good agreement with the experimental data with an error less than 10% (s. Table 3, Sim 4 & 5). For the fine packing 9M the CFD pressure drop is about 20% higher than the experiment and this difference increases

Table 3B. Dry pressure drop CFD-results

	F-factor	Exp. Δp	CFD Δp	^a turb. model	SS plates surfaces
	$Pa^{0.5}$	Pa/m	Pa/m		
Sim1	9M	1.09	45.2	56.0	rke-ewt wavy
Sim2	9M	2.18	150.2	194.7	rke-ewt wavy
Sim3	9M	4.36	498.3	750.5	rke-ewt wavy
Sim4	4M	1.09	25.0	25.0	rke-ewt wavy
Sim5	4M	2.18	85.0	92.9	rke-ewt wavy
Sim6	9M	2.18	150.2	237.4	rke-ewt flat-ver1
Sim7	9M	2.18	150.2	208.8	rke-ewt flat-ver2
Sim8	9M	2.18	150.2	256.7	rke-ewt flat-ver3
Sim9	4M	1.09	25.0	24.0	rke-ewt flat-ver1
Sim10	4M	2.18	85.0	88.9	rke-ewt flat-ver1

^arke: Realizable k- ϵ model, ewt: Enhanced wall treatment.

with the gas load (Sim 1 to 3). As can be seen, neglecting the fine plate texture with the small packing size leads to overprediction of the pressure drop and the embedding of the central node of the 4 lamellas in the grid with fine structure is decisive. However, at high gas flow rate the results are still not optimal. Further work with finer grid structure should resolve this problem.

CONCLUSIONS

In this work the hydrodynamics within structured packings and the rivulet flow on wavy plate were investigated with CFD methods. The rivulet profiles on a wavy plate were found in good agreement with the VOF simulations and the experimental liquid flow patterns on the packing sheet were found almost similar to that of the CFD simulations. The CFD simulations results on a single element have been exploited to develop a CFD-based correlations to describe the degree of wetting, specific interfacial area and liquid hold-up in Rombopak 4M, could, as has been shown, be validated on a multi-element packing sheet.

For coarse geometries (4M), the CFD simulations of dry pressure drops derived from plain lamellas were found in good agreement with the experiments. For fine textures, as is with 9M, it is important to correctly embed the structure in the CFD domain. As could be shown, CFD methods offer the potential to reveal the detailed flow structure of gas and liquid flow in complex packing geometries. This can be applied in optimization of the packing geometries and reveal critical details of wetting and film flow.

SYMBOLS USED

a	$[\text{m}^2/\text{m}^3]$	Specific packing surface area
a_h	$[\text{m}^2/\text{m}^3]$	Wetted surface area per unit volume
a_{ph}	$[\text{m}^2/\text{m}^3]$	Hydraulic (interfacial) surface area per unit volume
F-Factor	$[\text{Pa}^{0.5}]$	$u_g \rho_g^{1/2}$
g	$[\text{m}/\text{s}^2]$	Gravity
h_L	$[\text{m}^3/\text{m}^3]$	Liquid hold-up
u_L	$[\text{m}^3/\text{sm}^2]$	Superficial liquid velocity
u_g	$[\text{m}^3/\text{sm}^2]$	Superficial gas velocity

SUBSCRIPTS

h	Hydraulic (wetted)
g	Gas
L	Liquid

GREEK SYMBOLS

α	$[\text{°}]$	Plate inclination
θ	$[\text{°}]$	Contact angle
μ	$[\text{kg m/s}]$	Dynamic viscosity

ρ	[kg/m ³]	Density
σ	[N/m]	Surface tension
Δp	[Pa/m]	Pressure drop per unit length

DIMENSIONLESS NUMBERS

Fr_L	$(u_L^2 a/g)$	Liquid Froud number
Re_L	$(u_L \rho_L / a \mu_L)$	Liquid Reynolds number
We_L	$(u_L^2 \rho_L / a \sigma)$	Liquid Weber number

LITERATURE

1. V. V. Ranade (2002). *Computational fluid modeling for chemical reactor engineering*, Academic Press, San Diego.
2. P. Valluri, O. M. Matar, G. Hewitt and M. A. Mendes (2005). *Chem. Eng. Sci.*, 60 1965–1975.
3. L. Raynal, C. Boyer and J.-P. Ballaguet (2004). *Can. J. Chem. Eng.*, 82 (Aug.), 871–879.
4. A. Mohamed Ali, P. J. Jansens and Z. Olujic (2003). *Chem. Eng. Res. Des.*, 81 (Dec.), 108–115.
5. C. W. Hirt and B. D. Nichols (1981). *J. Comput. Phys.*, 39 201–225.
6. *FLUENT 6.2 User's Guide, 2005* Lebanon, NH 03766: Fluent Inc.
7. A. Hoffmann, I. Ausner, J.-U. Repke and G. Wozny (2004). *Chem. Ing. Tech.*, 75 (8), 1065–1068.
8. A. Hoffmann, I. Ausner, J.-U. Repke and G. Wozny (2005). *Comput. Chem. Eng.*, 29 1433–1437.
9. A. Ataki and H.-J. Bart (2004). *Chem. Eng. Technol.*, 27 (10), 1109–1114.
10. R. Billet and M. Schultes (1999). *Trans IChemE Part A*, 77 (Sep.), 498–504.
11. J. A. Rocha, J. L. Bravo and J. R. Fair (1993). *Ind. Eng. Chem. Res.*, 32 641–651.
12. J. A. Rocha, J. L. Bravo and J. R. Fair (1996). *Ind. Eng. Chem. Res.*, 35 1660–1667.
13. A. Ataki and H.-J. Bart (2002). Int. Conf. on Adsorption and Distillation, 634th event of the EFCE. VDI-GVC (ed.) 3-931384-37-3, Düsseldorf.
14. U. Bühlmann (1983). Rombopak, *Chem. Ing. Tech.*, 55 (5), 379–381.
15. L. Fischer, U. Bühlmann and R. Melcher (2003). *Trans IChemE, Part A*, 81, 79–84.
16. U. Bühlmann (1988). *Chemie-Technik*, 53 (4), 49–54.
17. A. Ataki and H.-J. Bart (2006). *Chem. Eng. Technol.*, 29 (3). In press.
18. G. D. Towell and L. B. Rothfeld (1966). *AIChE J.*, 12 (5), 972–980.
19. R. Billet (1995). *Packed Towers in Processing and Environmental Technology* VCH, Weinheim, Germany.